JOURNAL OF MATERIALS SCIENCE 30 (1995) 1180–1186

Nitridation characteristics of floating aluminium powder

AN-JAE CHANG, SHI-WOO RHEE*, SUNGGI BAIK
*Department of Materials Science and Engineering and *Laboratory for Advanced Materials Processing, Department of Chemical Engineering, Pohang University of Science and Technology, Pohang 790-784, Korea*

Experimental parameters for floating nitridation process were examined to study the effect on moving behaviour and direct nitridation characteristics of aluminium powder, which was carried over from a fluidized bed. The conversion increased with increasing reactor temperature and mole ratio of ammonia to aluminium. It was also strongly dependent on the thermal decomposition of ammonia participated in the reaction. Aluminium powder was converted to aluminium nitride as high as 0.90 when the reactor temperature was 1300 °C and the mole ratio was 19.5 The particle size and specific surface area of the powder increased with increasing conversion, which was due to the volumetric and structural change of aluminium particles when nitrided to form fine crystallites with higher porosity.

1. Introduction

Direct nitridation of aluminium is considered to be an attractive method for synthesizing aluminium nitride (AlN) powder. A large amount of powders could be manufactured with relatively low energy consumption, because the reaction is highly exothermic. Interparticle agglomeration during reaction, however, was the main problem in producing highly pure powder in the conventional 'static' process. A floating nitridation process (FNP) was recently developed to manufacture high quality AlN powder continuously and efficiently without coagulation [1]. Hotta *et al.* [2] synthesized fine and pure powder by nitridation of dispersed aluminium metal powder, which was carried over with a nitrogen gas stream. Kimura *et al.* [3] lowered the reaction temperature appreciably by introducing ammonia gas. Weimer *et al.* [4] reported the manufacturing of AlN powder with good quality by controlling thermophoresis with admixed inert powder, i.e. AlN or carbon powder. A major issue involved in FNP is to maximize the conversion to AlN giving the desired powder property.

The advantage of FNP is near-complete dispersion of powders, similar to an aerosol state, and hence the melting of aluminium powder does not lead to agglomeration. Reaction of aluminium metal with nitrogen or ammonia gas can be expressed as

$$Al + 1/2N_2 \rightarrow AlN \quad (1)$$

or

$$Al + NH_3 \rightarrow AlN + 3/2H_2 \quad (2)$$

Thermodynamically, the above two reactions have heats of formation at regions above room temperature (ΔH°_{298} is -318.0 and $-272.1\ kJ\ mol^{-1}$ for equations 1 and 2, respectively) [5]; and because of the exothermic heat, these reactions proceed non-isothermally, independent of the surrounding temperature [6]. Noticeable nitridation occurred only above the melting temperature of aluminium, as reported by Choi and Lee [7]. In spite of the high exothermic heat, an individual particle could not reach the theoretical adiabatic temperature (approximately 2800 K) [8], owing to the release of heat from the particle to surrounding gases. With the moving powder system, non-isothermal and extremely rapid reaction makes control difficult in comparison to static and isothermal process. Moreover, the properties of the produced powders may be largely influenced by the change of process conditions.

The purpose of present work is to examine the effect of process parameters on nitridation of aluminium powders entrained by a nitrogen gas stream containing ammonia. The behaviour of powders in the fluidized bed and free-board region was observed and characterized. The conversion was determined by X-ray quantitative analysis, and the powder characteristics, such as size distribution, specific surface area, powder morphology and the amount of unreacted aluminium metal, were also studied.

2. Experimental procedure

The experimental apparatus is shown in Fig. 1, and consists of parts for fluidization of aluminium powders, mixing and supplying of gases, reaction of floating particles and collection of product powders. The fluidizing vessel, with a gas distributor of 5 mm thick porous glass plate (pore size 100–150 μm), was connected to a quartz tube (inner diameter 4.2 cm, height 110 cm), which was fixed firmly in an electric furnace.

0022–2461

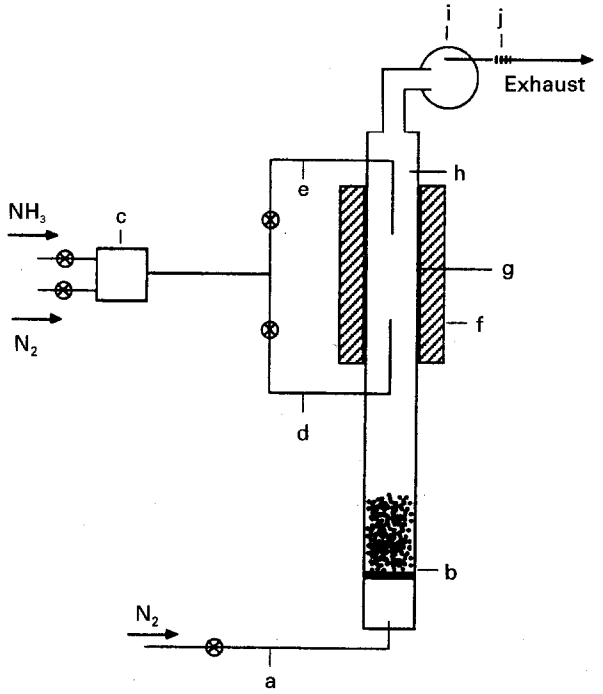

Figure 1 Schematic illustration of experimental apparatus: (a) carrier gas line, (b) powder fluidizing system, (c) gas mixing vessel, (d) concurrent feeding line, (e) counter-current feeding line, (f) electric furnace, (g) thermocouple, (h) reaction chamber, (i) collection vessel, and (j) paper filter.

TABLE I Characteristics of starting aluminium powder

Mean particle size, μm	24.6
Specific surface area, $m^2 g^{-1}$	0.45
Purity[a], %	99.9
Metal impurities[a], wt %	
Cu	0.0060
Fe	0.0700
Mg	0.0040
Mn	0.0070
Si	0.0600
Zn	0.0050
Oxygen content, wt %	0.3400
Nitrogen content, wt %	0.0083

[a] As provided by supplier.

TABLE II Typical operating condition for floating nitridation process

Process parameter	Experimental range
Temperature, °C	1000–1300
Flow rate of carrier gas, $l min^{-1}$	2.0
Feed rate of powder, $g min^{-1}$	0.037
Feed rate of mixture gas, $l min^{-1}$	1.0
Ammonia gas	0–0.9
Nitrogen gas	0.1–1.0
Feeding position of mixture gas[a], cm	
Concurrent direction	− 20 to + 10
Counter-current direction	− 10 to + 30

[a] Signs (+ , −) indicate the upper and lower position from the furnace centre, respectively.

Reagent grade aluminium powder (Al-110109, High-purity Chemicals Co.) was used as the raw material, and its characteristics are described in Table I. Nitrogen and ammonia gases, whose purities are above 99.99 and 99.999%, respectively, were used for carrying-over and nitridation of powders. To observe the fluidity and floating behaviour of powder, several tests were performed at room temperature prior to the reaction experiment.

Typical operating conditions for the reaction experiment are listed in Table II. The nitrogen carrier gas was supplied at a rate of $2.0 l min^{-1}$ and, in this case, the bed was fluidized smoothly with gas bubbles and some powder was floated vertically along with the gas stream. The feed rate of powder into the reaction chamber was determined from the rate of power consumption in the bed with running time. The reactor temperature and the mole ratio of ammonia to aluminium were varied from 1000 to 1300 °C and from 0 to 29.3, respectively. A mixture of ammonia and nitrogen was introduced into the centre of the reaction chamber through a concurrent feeding line [(d), Fig. 1]. To investigate the effect of ammonia introduction, gas feeding in a counter-current direction to the carrier gas was also tried.

Powders produced in different operating conditions were analyzed to measure the conversion and the powders' characteristics. Conversion was determined from the peak area ratio of the produced powder, and the calibration data were obtained from predetermined compositions of AlN and aluminium powders using an X-ray diffractometer (RAD-3C, Rigaku). The calibration curve shown in Fig. 2 reveals a good correspondence with the theoretical line, except for the

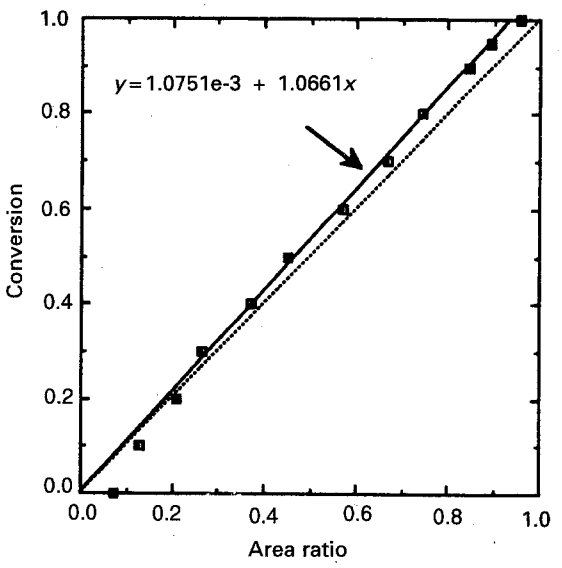

Figure 2 Calibration curve (——) for determining conversion from predetermined compositions of AlN and aluminium powders: (⊡) measured, (– – –) theoretical.

regions of higher and lower conversion. For above 0.80 and below 0.20, thus, conversion was determined from the oxygen and nitrogen contents, which were measured with an oxygen/nitrogen determinator (TC-436, Leco). Particle size distribution and specific surface area were measured with a particle size analyser (Granulometer HR 850, Cilas-Alcatel) and by the Brunaver–Emmett–Teller (BET) method (AccuSorb 2100E, Micrometrics), respectively. The morphology

of the powder was observed with a scanning electron microscope (S-570, Hitachi) and the impurities were determined by atomic absorption spectroscopy (5100 PC, Perkin–Elmer). In order to differentiate AlN with unreacted free aluminium metal resided in the powders, following light grinding the samples were subjected to thermogravimetric analysis.

3. Results and discussion

3.1. Moving behaviourof floating powder

Fluidization is the operation by which fine solids are transformed into a fluidlike state through contact with a gas or liquid. Gas–solid systems generally behave in quite different manners, with bubbling or channelling of gas compared to liquid–solid systems. According to Geldart [9], the mode of a gas–solid fluidized bed depends on the density difference and mean particle size. Generally, small particles are classified as group C powders, which are very adhesive and hard to fluidize. Many workers have studied the nature of fluidization for group C powders and found good fluidity by controlling those factors such as bed geometry, gas flow rate, type of gas distributor and species of particles [9–11].

Fluidization in the present work was hard to achieve because of the fine size of the powders. Fluidization was observed at $> 0.5\,l\,min^{-1}$ of carrier gas after shaking the bed severely. Particle entrainment started from about $1.0\,l\,min^{-1}$ of carrier gas. Fig. 3 shows powder consumption in the bed as a function of running time, which has a constant rate of 0.053 and $0.037\,g\,min^{-1}$ at $2.0\,l\,min^{-1}$ of carrier gas, when 100 and 50 g of powder was loaded, respectively. Fig. 4 shows the particle size distribution of powders after running for 1 h at room temperature: the solid line represents the starting powder, and the dotted lines represent the floated and remaining aluminium powders. All the powders have Gaussian or normal distributions, and only powder $< 15\,\mu m$ in diameter could

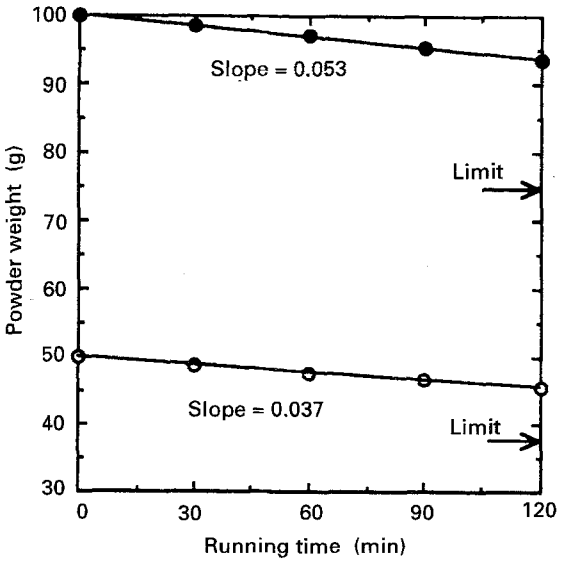

Figure 3 Consumption of powder in a bed as a function of running time when the carrier gas flowed at $2.0\,l\,min^{-1}$ and the powder was loaded as (●) 100 and (○) 50 g samples, respectively; the slopes represent the powder feed rates in $g\,min^{-1}$.

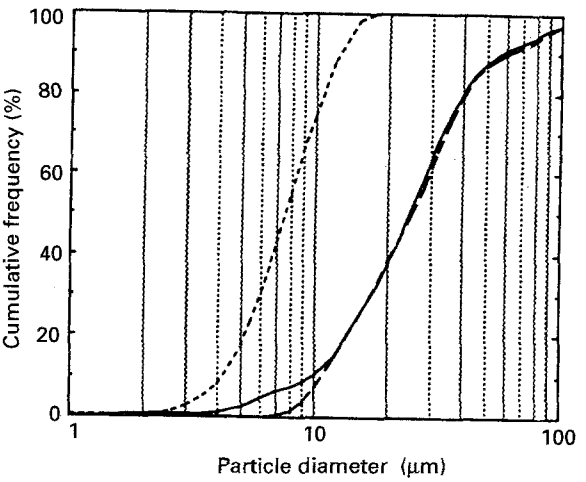

Figure 4 Particle size distribution of powder which was (---) floated to the collection vessel and (—·—) remained in the fluidizing vessel after running for 1 h at room temperature. (——) starting powder.

be floated and accumulated at the collection vessel. By theoretical calculation for the solid particle–gas system, the behaviour of the floating particle can be estimated. Superficial gas velocity, u_o, in the reaction tube is $2.0\,cm\,s^{-1}$, calculated from the gas flow rate divided by the cross-sectional area of the tube. The terminal velocity or free-fall velocity, u_t, for a particle of diameter, d_p, when the Reynolds number, Re_p ($= d_p u_o \rho_g/\mu$), is below 0.4, is [9]

$$u_t = g(\rho_s - \rho_g)d_p^2/(18\,\mu) \quad (3)$$

where ρ_s is the density of the solid ($2.7\,g\,cm^{-3}$); ρ_g, the density of the gas ($12.5 \times 10^{-4}\,g\,cm^{-3}$); μ, the viscosity of the gas ($1754 \times 10^{-7}\,g\,cm^{-1}\,s^{-1}$); and g, gravitational acceleration. The value of u_t, for a mean particle size of $7.6\,\mu m$ is $0.48\,cm\,s^{-1}$. From the terminal velocity, calculation of critical size, which separates the particles carried by the gas stream ($u_t < u_o$) from those returning to the bed ($u_t > u_o$), is possible [12]. The maximum size of a floating particle is $15.4\,\mu m$, and this is consistent with the experimental value. The theoretical limit of floatable powder is calculated to be about 25% of the starting powder.

At a sufficiently high flow rate above the terminal velocity of the solids, entrainment becomes appreciable and solids are carried out of the bed with the fluid stream. Particle velocity, v_p, therefore, is the difference between the superficial fluid velocity and the particle terminal velocity [12], that is

$$v_p = u_o - u_t = u_o - 83.8 \times 10^4 d_p^2 \quad (4)$$

Residence time, t_r, for the floating particle in the reaction zone (when uniform length, l_o, is 30 cm) is therefore

$$t_r = l_o/v_p = 30/(u_o - 83.8 \times 10^4 d_p^2) \quad (5)$$

Fig. 5 shows the theoretical calculation curves for particle velocity and residence time as a function of particle diameter at a superficial gas velocity of

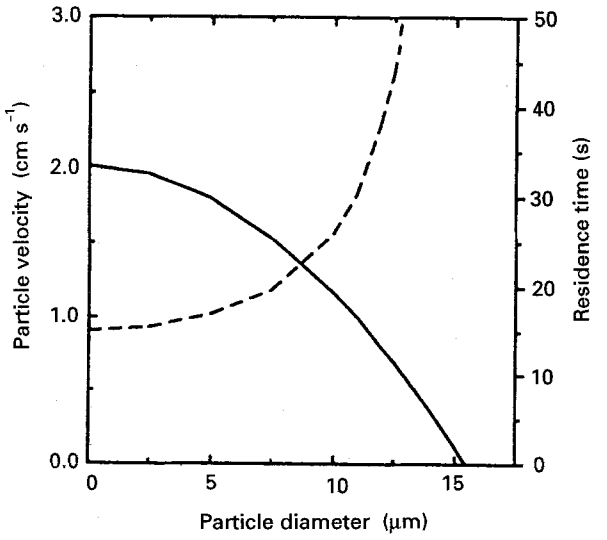

Figure 5 Curves drawn by theoretical calculations for (——) particle velocity and (– –) residence time as a function of particle diameter.

2.0 cm s^{-1}. Values of v_p and t_r are dependent on the particle size distribution as well as on the superficial gas velocity. The average particle velocity and residence time for a median particle diameter of 7.6μm were calculated to be 1.52 cm s^{-1} and 19.7 s, respectively.

3.2. Process parameters and conversion ratio

Fig. 6 shows X-ray diffractograms for the powders formed at various reactor temperatures and mole ratios of ammonia to aluminium for the typical operating condition. At elevated temperature, with a constant mole ratio of 19.5 (Fig. 6a–d), aluminium peaks became smaller and AlN peaks grew bigger when the reactor temperature was between 1000 and 1300 °C. With increasing mole ratio at 1200 °C, Fig. 6e–h, conversion increased considerably, but the aluminium peak appeared again at the highest mole ratio of 29.3.

Fig. 7 shows conversion as a function of reactor temperature at an ammonia feed rate of 0.6 l min^{-1} and at a powder feed rate of 0.053 or 0.037 g min^{-1}. The conversions at 1000 °C were 0.14 and 0.38 for each powder feed rate, and the increase of reactor temperature raised the conversion up to 0.90. The powder feed rate also had a considerable effect on conversion and on the temperature needed for maximum conversion.

Fig. 8 shows the conversion as a function of NH_3/Al mole ratio for two different powder feed rates as shown in Fig. 7, in which the reactor temperature was fixed at 1200 °C. Without the introduction of ammonia, little conversion (below 0.01) was observed and, as the mole ratio increased, the conversion increased until it became saturated at 0.87 at > 15. The decrease in conversion at the highest mole ratio of 29.3 can be attributed to the temperature drop, due to the

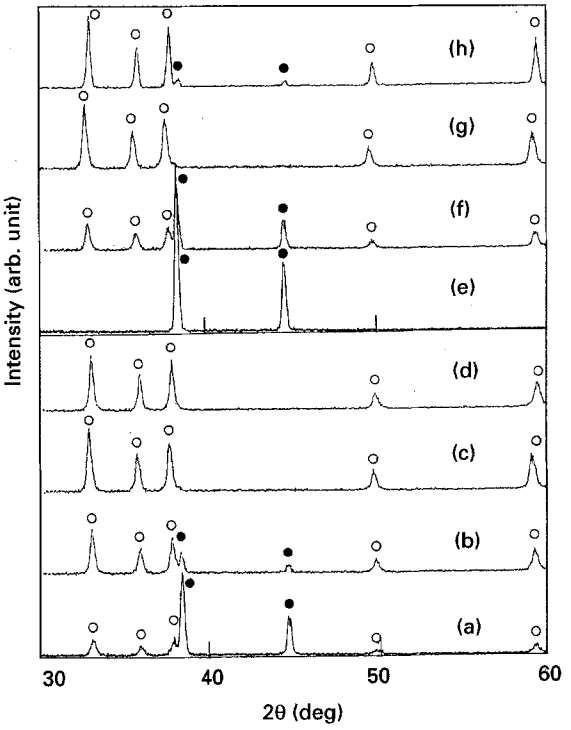

Figure 6 X-ray diffraction patterns of the powders formed at reactor temperatures of (a) 1000, (b) 1100, (c) 1200, and (d) 1300 °C (NH_3/Al mole ratio was 19.5); and at NH_3/Al mole ratio of (e) 0, (f) 9.8, (g) 19.5 and (h) 29.3 (reactor temperature was 1200 °C), respectively: (●) aluminium, (○) AlN.

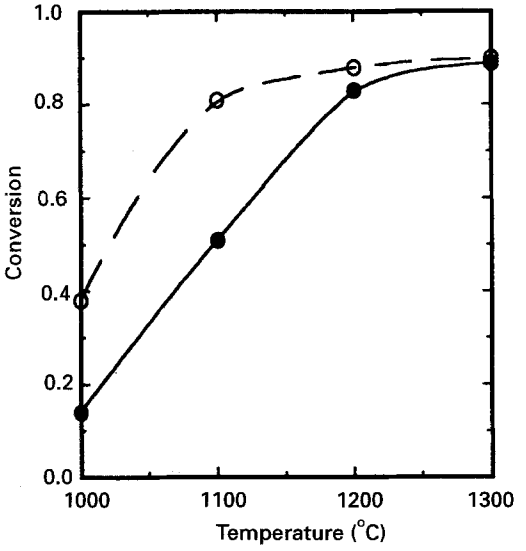

Figure 7 Conversion of powders as a function of reactor temperature: powder feed rates were (●) 0.053 and (○) 0.037 g min^{-1} (NH_3/Al mole ratio of 13.6 and 19.5), respectively.

dissociation of extra ammonia gas according to

$$NH_3 = 1/2N_2 + 3/2H_2 \qquad \Delta H^\circ_{298} = 45.9\ \text{kJ mol}^{-1} \qquad (6)$$

To investigate the effect of ammonia thermal decomposition on conversion, the feeding position and direction were varied from the typical operating mode, in which ammonia was introduced at the centre of the reactor with concurrent direction. The reactor temperature and NH_3/Al mole ratio were 1200 °C and 13.6,

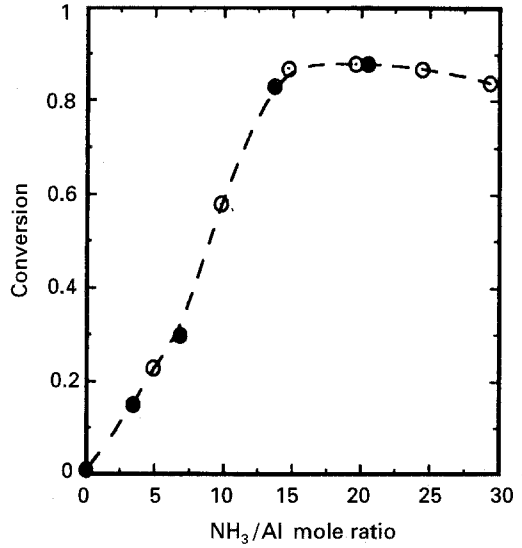

Figure 8 Conversion of powders as a function of NH_3/Al mole ratio: powder feed rates were (●) 0.053 and (○) 0.037 g min^{-1}, respectively, (reactor temperature was 1200 °C).

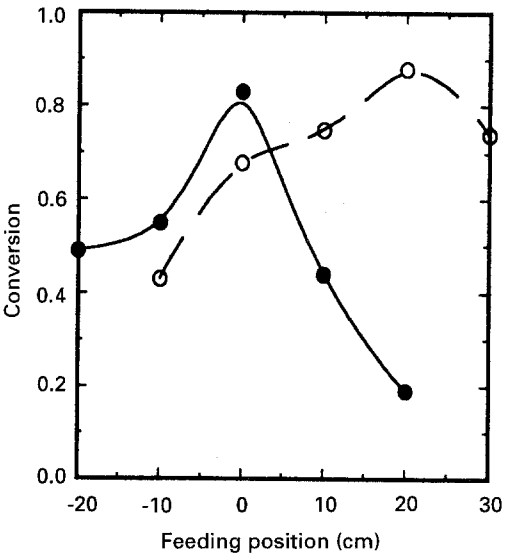

Figure 9 Conversion of powders as a function of ammonia feeding direction and position: ammonia mixture gas was fed to (●) concurrent and (○) counter-current direction to carrier gas stream (reactor temperature was 1200 °C and NH_3/Al mole ratio was 13.6).

respectively. As shown in Fig. 9, there exists a large difference in conversion due to a slight change of ammonia feeding position; this was also found by Kimura *et al.* previously [3]. The higher conversion obtained with the reverse feeding direction is thought to be due to the effective mixing and longer contact time of floating powder with ammonia mixture gas induced as a counter-currently flowing fluid. However, this could also be due to a decrease in the dissociation of ammonia. Ammonia or its radicals are highly reactive with aluminium at high temperatures, but they decompose easily and rapidly at temperatures as low as 130 °C [13] by Equation 6. Nitrogen is not so reactive as ammonia and does not react readily with aluminium. In the reaction of ammonia with aluminium chloride ($AlCl_3$), it was reported that almost complete conversion of $AlCl_3$ to AlN was possible by suppressing the dissociation of ammonia [14, 15].

3.3. The powders' properties

Oxygen and nitrogen contents of the produced powders are listed in Table III. The nitrogen contents show the same trend as shown in Figs 7 and 8, and the oxygen contents were lower than the commercial AlN powder manufactured by conventional direct nitridation methods (F-grade, Toyo Aluminum). But the nitrogen content was not higher than the theoretical value (34.2%), even for the powder experiencing maximum conversion. This suggests that unreacted aluminium still remained in the powder produced.

The particle size of the powders were changed with different operating conditions, as shown in Fig. 10. As the mole ratio of NH_3/Al was elevated from 0 to 29.3, the median diameter of the powder was changed from 9.2 to 14.3 μm. This may be due to the volume change of aluminium particles in AlN. The molar volume change, V^m_{AlN}/V^m_{Al}, was calculated to be 1.32. The observed value from the change of a particle's median diameter, showed a volume change of 3.72. This discrepancy could be explained from the results of BET and microstructural analyses.

TABLE III Oxygen/nitrogen contents of powders formed at various conditions

Temperature (°C)	NH_3/Al (mol mol^{-1})	Oxygen (wt %)	Nitrogen (wt %)
1200	0.0	0.72	0.21
1200	9.8	1.17	19.40
1200	19.5	1.08	29.30
1200	29.3	1.08	28.10
1000	19.5	1.75	11.90
1100	19.5	1.70	27.00
1300	19.5	1.06	30.20
Reference[a]	–	1.76	31.30

[a] Commercial AlN powder manufactured by direct nitridation method.

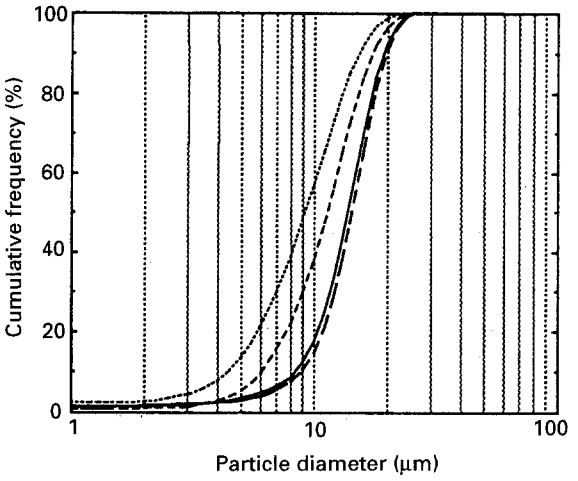

Figure 10 Particle size distribution of powders formed at 1200 °C and NH_3/Al mole ratio of (·····) 0, (---) 9.8, (– –) 19.5 and (——) 29.3, respectively.

Depending on the mole ratio of NH_3/Al at 1200 °C, the produced powders showed a large difference in specific surface area, as represented in Table IV. With increasing conversion, the surface area increased

TABLE IV Specific surface areas of powders formed at 1200 °C and various mole ratio of NH_3/Al

NH_3/Al (mol mol^{-1})	Surface area ($m^2 g^{-1}$)	Conversion ratio[a]
0.0	0.81	0.01
9.8	15.10	0.58
19.5	23.10	0.88
29.3	18.70	0.84

[a] Determined by oxygen and nitrogen contents.

appreciably, which suggests that there was a considerable change in particle shape. The surface area decreased again at the highest mole ratio of 29.3, which may have been caused by the microstructural change of particles, rather than by a conversion change, because its conversion was similar to the powder formed at a mole ratio of 19.5.

The electron micrographs shown in Fig. 11 strongly support the previous results. With increasing mole

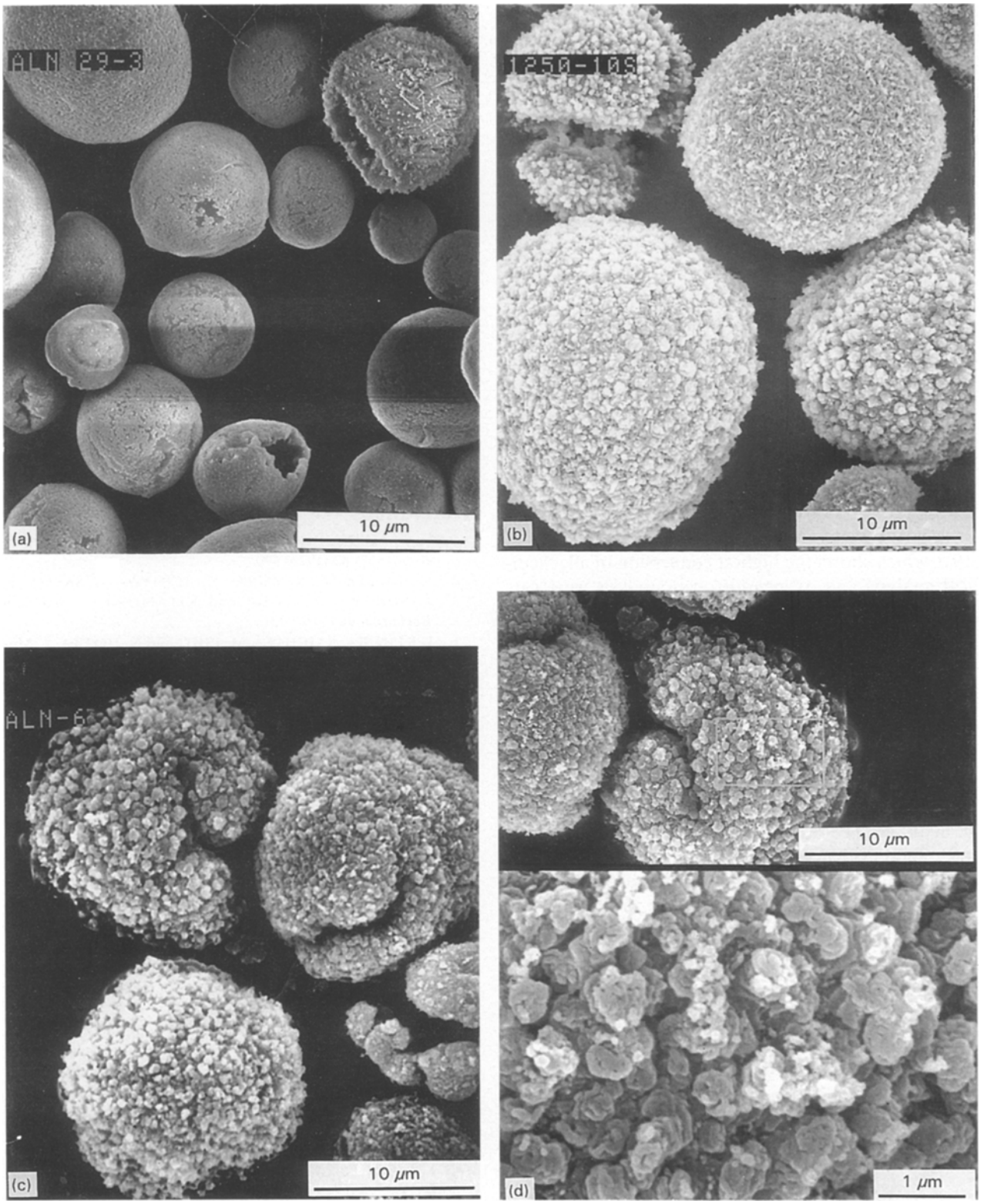

Figure 11 Scanning electron micrographs of powders formed at 1200 °C and NH_3/Al mole ratio of (a) 0, (b) 9.8, (c) 19.5, and (d) 29.3, respectively.

TABLE V Chemical compositions of powders formed at 1300 °C and NH_3/Al mole ratio of 19.5

Elements	Contents (wt %)	Reference[a] (wt %)
Al	65.31	64.8300
N	30.200	31.3000
O	1.060	1.7600
Cu	0.014	0.0088
Fe	0.085	0.0400
Mg	0.016	0.0180
Si	0.250	Trace

[a] Commercial AlN powder manufactured by direct nitridation method.

ratio, particle shapes changed and their surfaces became rough. For unconverted powder with no ammonia introduced, most of the particles (primary particles) had smooth surfaces, and a "crater-like" shape was found in some particles, as Hotta *et al.* had observed [2]. For partially converted powders at a lower mole ratio of 9.8, all the primary particles became bigger and covered with fine nitrided crystallites (secondary particles). For highly converted powders at a higher mole ratio of 19.5, most of the primary particles had a porous structure, and consisted of secondary particles with increased size. Cracks in the primary particles were though to be due to the nitridation of core aluminium melt accompanying volume expansion during the reaction. For the highest mole ratio of 29.3, the crystallites were larger than before, which is consistent with the results of BET analysis (Table IV). The increase in size of the secondary particles is due to the growth of nucleates on the reaction sites, as already discussed [16].

For the powder formed at 1300 °C and mole ratio of 19.5, which shows the highest conversion of all, chemical analysis and oxygen/nitrogen analysis were carried out to determine the amounts of impurities and unreacted aluminium. As shown in Table V, the metallic and oxygen impurities were as low as the starting aluminium powder and the commercial-grade AlN powder used as a reference. However, the aluminium content was higher than that of the reference powder, while the amount of nitrogen was not; which indicates that several per cent of unreacted free aluminium still remained and complete conversion to AlN could not be achieved. The results of thermogravimetric analysis gave good evidence for free aluminium; the saturated weight gain at 1500 °C for 3 h in a nitrogen atmosphere was 4.2%. This is quite close to the value of 4.8% for the nitridation of 9.3% free aluminium, which was calculated from stoichiometric AlN and Al_2O_3.

4. Conclusions

From the experiment for rapid direct nitridation of floating aluminium powders, the following conclusions were obtained.

1. The powder feed rate out of the fluidizing bed and the critical size of floatable particles could be controlled by the amount of loaded powder in the bed and the flow rate of the carrier gas, respectively. The values of moving velocity and residence time of powders are dependent on the superficial gas velocity and the particle size distribution.

2. Increasing the reactor temperature from 1000 to 1300 °C raised the conversion of powders, but complete conversion to AlN could not be achieved.

3. Without the introduction of ammonia, little conversion was obtained at 1200 °C, and as the mole ratio of ammonia to aluminium increased, the conversion went up appreciably. However, the supply of excess ammonia could lower the conversion because of the temperature drop due to the dissociation of extra ammonia.

4. Variation of feeding direction and position of ammonia in the reaction chamber had a considerable influence on the conversion, and this is due to the change in contact time of aluminum powder with ammonia gas and to the thermal decomposition of ammonia.

5. The size and shape of the particles produced were affected by the experimental conditions. With increasing conversion by the elevating mole ratio of ammonia to aluminium, the primary particles became bigger and more porous, while the secondary particles, which covered the surface, increased in size.

Acknowledgements

This work was supported by the Research Institute of Science and Technology (RIST). We are grateful to Dr Yoon Choi for valuable discussion and also thank Mr Won-soo Pae for several analyses.

References

1. S. MATSUO, N. HOTTA and Y. NISHWAKI, *Yogyo-Kyokai-Shi* **83** (1975) 490.
2. N. HOTTA, I. KIMURA, K. ICHIYA, N. SAITO, S. YASUKAWA, K. TODA and KITAMURA, *Seramikkusu Ronbunshi* **96** (1988) 731.
3. I. KIMURA, K. ICHIYA, M. ISHII and N. HOTTA, *J. Mater. Sci. Lett.* **8** (1989) 303.
4. A. W. WEIMER, G. A. COCHRAN, G. A. EISMAN and J. P. HENLEY, *Aero. Sci. Technol.* **19** (1993) 491.
5. M. W. CHASE, JR, C. A. DAVIES, J. R. DOWNEY, JR, D. J. FRURIP, R. A. MCDONALD and A. N. SYVERUD, in "JANAF Thermochemical Tables", 3rd Ed (American Institute of Physics, New York, 1986).
6. S. ITO, I. EBATO, H. FUKUI, N. KOURA and N. YONEDA, *J. Ceram. Soc. Jpn.* **100** (1992) 629.
7. S. CHOI and S. LEE, *J. Kor. Ceram. Soc.* **22** (1985) 80.
8. J. SUBRAHMANYAM and M. VIJAYAKUMAR, *J. Mater. Sci.* **27** (1992) 6249.
9. D. KUNII and O. LEVENSPIEL, "Fluidization Engineering" (Wiley, New York, 1969) p 64.
10. J. F. DAVIDSON, R. CLIFT and D. HARRISON, "Fluidization" (Academic Press, London, 1985) p. 39.
11. S. MOROOKA, K. KUSAKABE, A. KOBATA and Y. KATO, *J. Chem. Eng. Jp.* **21** (1988) 41.
12. F. A. ZENZ and D. F. OTHMER, "Fluidization and Fluid-Particle Systems" (Chapman & Hall, London, 1960) p. 374.
13. D. R. GASKELL, "Introduction to Metallurgical Thermodynamics", 2nd Edn (McGraw-Hill, New York, 1981) p. 248.
14. K. G. NICKEL, E. RIEDEL and G. PETZOW, *J. Amer. Ceram. Soc.* **72** (1989) 1804.
15. J. PARK, S. RHEE and K. LEE, *J. Mater. Sci.* **28** (1993) 57.
16. A. CHANG, S. BAIK and S. RHEE, *J. Amer. Ceram. Soc.* in press.

Received 11 April
and accepted 6 July 1994